Hydrol. Earth Syst. Sci. Discuss., 8, 11357–11385, 2011
www.hydrol-earth-syst-sci-discuss.net/8/11357/2011/
doi:10.5194/hessd-8-11357-2011

Hydrology and Earth System Sciences Discussions

Satellite remote sensing of water turbidity in Alqueva reservoir and implications on lake modelling

M. Potes[1], **M. J. Costa**[1,2], **and R. Salgado**[1,2]

[1]Évora Geophysics Centre (CGE), University of Évora, Rua Romão Ramalho 59, 7000-671 Évora, Portugal
[2]Department of Physics, University of Évora, Rua Romão Ramalho 59, 7000-671 Évora, Portugal

Received: 7 October 2011 – Accepted: 11 December 2011 – Published: 21 December 2011

Correspondence to: M. Potes (mpotes@uevora.pt)

Published by Copernicus Publications on behalf of the European Geosciences Union.

Abstract

The quality control and monitoring of surface freshwaters is crucial, since some of these water masses constitute essential renewable water resources for a variety of purposes. In addition, changes in the surface water composition may affect physical properties of the lake water, such as temperature, which in turn may impact exchanges with the lower troposphere.

The use of satellite remote sensing to estimate water turbidity of Alqueva reservoir, located in the south of Portugal, is explored. A validation study of the satellite derived water leaving spectral reflectance is firstly presented, using data taken during three field campaigns carried out during 2010 and early 2011. Secondly an empirical algorithm to estimate lake water surface turbidity from the combination of in situ and satellite measurements is proposed. The importance of water turbidity on the surface energy balance is tested in the form of a lake model sensitivity study to the water extinction coefficient (estimated from turbidity), showing that this is an important parameters tuning the lake surface temperature.

1 Introduction

Climate seasonality is the most relevant natural temporal change, particularly rainfall and solar heating, resulting in seasonal variations in water quality (Chapman, 1996). A better understanding of the characteristics of reservoirs systems such as physical and chemical properties of water and hydraulics is essential to sustain these important fresh-water resources (Lee, 1997). Water quality of reservoirs is determined by several factors, thus, the success of a reservoir management depends on the detection of spatial and temporal changes in reservoir status that reflect natural and anthropogenic alterations in the surrounding environment (Morais et al., 2007). Turbidity is an optical property of the water body – a measure of the amount of light scattered and absorbed by particles in the water sample (Michaud, 1991). The water turbidity is related with

HESSD

8, 11357–11385, 2011

Satellite remote sensing of water turbidity in Alqueva reservoir

M. Potes et al.

extinction of light in water and consequently with thermal vertical structure of the lakes, which in turn plays an important role in autochthonous primary production (Friedl and Wüest, 2002).

In general, light intensity declines exponentially with depth, as described by Beer-Lambert Law:

$$I_Z = I_0 e^{-kz} \quad (1)$$

where I_Z is the light intensity at a depth z below the surface, I_0 is the immediate sub-surface light intensity, Z is the depth interval between I_0 and I_Z and k is the rate of attenuation of downwelling radiation usually referred to as the extinction coefficient.

According to Moore (1980), the feasibility of measuring water color and turbidity from satellites can be assessed by considering light and water interaction processes and by evaluating the effects of atmospheric and hydrological variables. The use of satellite data to evaluate the optical water properties is steadily increasing, since this kind of data provides undoubtedly the only way to proceed for global characterization of the reservoirs (Koponen et al., 2002; Chen et al., 2006; Gons et al., 2008; Alikas and Reinart, 2008; Duan et al., 2008; Gitelson et al., 2008; Tyler et al., 2006; Simis et al., 2007). Note that the many Low Earth Orbit satellite instruments launched in the last decade constitute exceptionally valuable tools for surface water quality quantitative analysis (Dickey et al., 2006). Their multi-spectral and spatial resolution capabilities allow for improved techniques in retrieving the lake water optical properties. A good example is the MEdium Resolution Imaging Spectrometer (MERIS), onboard ENVISAT satellite, which combines moderately high spatial resolution ($300 \times 300\,m^2$ at nadir) with an adequate spectral resolution in the visible and near infra-red (ESA, 2006). Higher spatial resolution satellite systems are available, but there are difficulties associated with their use: on one hand their rare frequencies over the same area and on the other hand, the related expenses. The use of MERIS represents a good compromise in order to have low-cost frequent (nominal revisit time of 2–3 days at midlatitudes) monitoring of inland water bodies.

HESSD
8, 11357–11385, 2011

The present work aims at demonstrating the possibilities and potential of using satellite remote sensing data to obtain information on lake water turbidity, which is essential for the improved use of lake schemes introduced in weather forecast and climate models.

Potes et al. (2011) recently developed a method to retrieve surface freshwater biological parameters (chl-*a* and cyanobacteria) concentrations over Alqueva reservoir (south of Portugal) from MERIS satellite data, aiming at providing full spatial coverage and continuous monitoring of these parameters that affect the water quality. The methodology is now adapted and presented here to obtain a new empirical algorithm allowing retrieving the water turbidity of the same reservoir, which is important for the estimation of water extinction coefficients. The assessment of the reliability of the retrievals is highly dependent on the comparison with independent measurements that allow for error estimation and eventually achieve a validation of the method (Dickey et al., 2006). The basis of the methodology is the atmospheric correction accuracy, for that reason an extensive database of water leaving spectral reflectance (Gordon and Wang, 1994) is being collected for Alqueva reservoir, since 2010, in correspondence of satellite overpasses, in order to achieve validation of the atmospheric correction methodology proposed. The first results of this validation are also presented here.

Turbidity is an important parameter that may induce changes in lake properties, namely on parameters such as the water temperature, which may in turn have important effects on the atmospheric boundary layer. Lakes strongly affect the structure of the atmospheric boundary layer and therefore the weather and the climate on a variety of scales. However, until very recently, the weather forecast models did not include an explicit representation of the evolution of lake properties. Currently, many efforts are being made to include 1-D lake schemes in operational numerical weather prediction (NWP) models (e.g. Mironov et al., 2010; Salgado and Le Moigne, 2010; Dutra et al., 2010). The two layer bulk lake model, FLake (Mironov, 2008), enjoys growing popularity in NWP and climate models as well as in limnology.

HESSD
8, 11357–11385, 2011

In order to incorporate a lake parameterization scheme into a NWP or climate model, a number of two-dimensional external parameter fields are required, in particular those describing the optical proprieties of the water bodies. The FLake model includes the following optical parameters: surface albedo, long wave emissivity and light extinction coefficient. The water extinction coefficient is rarely measured directly. On the contrary, turbidity is frequently measured in many lakes and reservoirs, since it is included in the water quality monitoring programs. There are some studies aiming at relating turbidity measurements with extinction coefficients (Giblin et al., 2010; Parkhill and Gulliver, 2002), nevertheless these relationships depend on the water mass conditions, therefore more studies for several different environments are required to truthfully determine water extinction coefficients from turbidity measurements. The use of satellite data may be the best choice in order to derive global maps of the water extinction coefficient making use of the turbidity-extinction coefficient relationships.

The importance of the water mass optical characteristics, in this case represented by the extinction coefficient, is evidenced through a sensitivity study of the water surface temperature and water-atmosphere heat fluxes evolution to the extinction coefficient, carried out using the FLake model and presented here.

The aim of the present work is twofold: firstly it endeavors at developing a satellite-based remote sensing method to retrieve surface inland freshwater turbidity, which is a measure of water quality characterizing its optical behavior and deemed an essential parameter towards the improvement of lake schemes in weather forecast and climate models; secondly and as a natural consequence of the previous aim, it is objective of the work to show the importance of the lake optical characteristics in the evolution of lake surface temperature and heat fluxes. This is done through a sensitive analysis of lake model results to different values of the extinction coefficient, representing here possible extreme water turbidity cases.

The following section gives a description of the data and method used. Sections 3 and 4 present the results and Sect. 5 summarizes the conclusions.

HESSD
8, 11357–11385, 2011

2 Data and method

The Alqueva reservoir, located in the south of Portugal along 83 km of the main course of the Guadiana River, constitutes the largest artificial lake on the Iberian Peninsula (Fig. 1). At the full storage level of 152 m, the reservoir has a total capacity of 4150 km^3 and a surface area of 250 km^2. Filling of Alqueva reservoir began in February 2002 and lasted about one year to reach a stable storage level of about 135 m.

According to Morais et al. (2007), Alqueva reservoir was classified as eutrophic based on total phosphorus and chl-*a* concentrations. The Alqueva water quality control belongs to a large monitoring programme implemented by the Portuguese company responsible for Alqueva exploitation (Empresa de Desenvolvimento e Infra-Estruturas de Alqueva, EDIA). The monitoring programme was implemented at the beginning of the filling phase. Nevertheless, this control is spatially and temporally limited. Monthly water samples are collected, and afterwards analyzed in laboratory, in a few spots of the reservoir. Two sites were selected (up to 500 m from the shore) for the validation presented in this study, taking into account not only their geographical positions inside the reservoir, but also the corresponding satellite image pixel dimension (300×300 m^2) that should enclose an homogeneous surface. Figure 1 illustrates the location of these sites, namely Mourão and Montante. This selection aims, in addition, to reduce as much as possible the adjacency effects, consisting on the brightening of dark water pixels due to reflections from neighboring land (vegetation or soil) pixels, with higher reflectances, which reach the sensor and appear to come from a water pixel, reducing the contrast between water and land pixels.

Since March 2002, with the launch of ENVISAT (ENVIronmental SATellite) by the European Space Agency (ESA), an advanced polar-orbiting Earth observation satellite provides measurements of the atmosphere, ocean, land, and ice, supporting Earth science research and monitoring the evolution of environmental and climate changes. ENVISAT satellite flies in a sun-synchronous polar orbit of about 800 km altitude, with

HESSD
8, 11357–11385, 2011

repeat cycle of the reference orbit is 35 days, and for most sensors included in this satellite, being wide swath, it provides a complete coverage of the globe within one to three days.

The Medium Resolution Imaging Spectrometer (MERIS), onboard ENVISAT, is a 68.5° field-of-view push-broom imaging spectrometer that measures the solar reflected radiation from the Earth, ranging from the visible to the near infrared (400 to 1040 nm), with programmable spectral band position and width between 2.5 and 20 nm (http://earth.esa.int/envisat/instruments/meris/descr/concept.html, last accessed 12 April 2011). These spectral bands were carefully chosen in accordance with the mission goals and priorities of MERIS instrument, to ensure practical applicability of the sensor. A wide swath of 1150 km is observed thus achieving global coverage within three days. Full spatial resolution data is 300 m at nadir and reduced spatial resolution data is achieved by onboard combination of 4 × 4 adjacent pixels across-track and along-track resulting in a resolution of approximately 1200 m at nadir.

MERIS calibration is performed at the orbital South Pole, when a reference diffuser is illuminated by the Sun. During calibration, the Earth-view port is closed and the sun-view port opened to provide, in the case of radiometric calibration, a uniform radiance source, and in the case of spectrometric calibration, a radiance source with a spectral signature. The reference for the absolute calibration is based on an assumed solar irradiance at the time of the calibration. The radiance is adjusted from this reference by applying appropriate seasonal scaling.

MERIS full resolution (FR) level 1 imagery are used, corresponding to spectral top of the atmosphere (TOA) radiances for each of the MERIS spectral channels, with the maximum spatial resolution of 300 × 300 m^2 at the nadir. The selection of the MERIS images was based on three conditions: (i) minimum time lag between MERIS and limnological sampling dates due to possible alterations of the water surface parameters (one day difference); (ii) cloud-free conditions (MERIS cloud mask); (iii) lack of aerosol events (generally desert dust or forest fire smoke). A water mask is applied to identify inland waters pixels from Alqueva reservoir. The test relies on the TOA (top of the atmosphere) spectral reflectances, with the condition that band 6 (620 nm) > band 10 (753.75 nm) and band 13 (865 nm) < 0.1.

2.1 Atmospheric correction validation

The study of surface water properties from satellite remote sensing techniques requires the correction of the atmospheric effects. The present study is applied only to cloud-free days over Alqueva reservoir. Major gas absorption bands are avoided as well, therefore, the atmospheric correction depends essentially on the type and amount of aerosols present in the atmosphere. Aerosol event situations are also discarded, being considered only clean background aerosol conditions (Elias et al., 2006). A comprehensive description of the atmospheric correction methodology used is given by Potes et al. (2011). The aerosol measurements (optical thickness, size distribution, and complex refractive index) continuously taken at the observatory of the Évora Geophysics Centre (CGE), as part of the AErosol RObotic NETwork (AERONET) (Holben et al., 2001), are used in the atmospheric correction. This is done assuming that there isn't a significant variation in the aerosol conditions between Évora and Alqueva area (horizontal distance of about 50 km), which most of the time is an accurate approximation, except in case of aerosol events (Elias et al., 2006). The second simulation of the satellite signal in the solar spectrum (6S) radiative transfer model (Vermote et al., 1997) is adopted for the atmospheric correction. The 6S can simulate satellite radiation measurements in cloud-free atmospheres, between 0.25 and 4.0 µm, for a wide range of atmospheric and surface conditions, taking into account the main atmospheric compounds, considering 34 atmospheric levels distributed from the ground up to 100 km altitude. The adjacency effects due to reflection from contiguous pixels are also taken into account in the algorithm, considering water, vegetation or soil surface, according to the neighbouring pixel classifications (Potes et al., 2011).

During 2010 and 2011 three field campaigns were carried out in Alqueva reservoir, to measure water leaving spectral reflectance, with the aim of validating the satellite atmospherically corrected spectral reflectance. A portable spectroradiometer (FieldSpec

HESSD
8, 11357–11385, 2011

UV/VNIR) from ASD Inc. was used for this purpose and the water leaving spectral reflectance was measured across the spectral range 325–1075 nm with 1 to 3 nm spectral resolution from visible to near infrared. The campaigns took place during the mornings of 27 July 2010, 25 August 2010 and 24 February 2011, with measurements taken before, during and after the ENVISAT overpasses in the region.

Figure 2 shows a comparison between the measured and satellite-derived water leaving reflectance spectra for 25 August 2010. The measured spectrum is identified as FieldSpec (solid line) and it corresponds to the average of ten measured spectra. The different satellite-derived spectra correspond to the: (i) atmospheric correction developed by the authors (Potes et al., 2011), hereinafter referred to as MERIS L1 + 6S; (ii) MERIS level 1b lake algorithm (Doerffer and Schiller, 2008), referred to as MERIS ATBD; (iii) MERIS level 2, identified as MERIS L2. To note that the atmospheric correction scheme developed by the authors (MERIS L1 + 6S) is the one that better matches the measured water leaving reflectance for the three campaigns carried out (only shown here for 25 August 2010).

Figure 3a presents a scatter plot of the measured versus satellite-derived water leaving spectral reflectance, obtained for the three field campaigns carried out. The three campaigns may be distinguished by the different symbols and the statistical parameters of the regressions obtained for each of the campaigns, considering the MERIS L1 + 6S retrieval and the field measurements, are shown in Table 1. On 25 August 2010 a good agreement between ground-based measurements and satellite retrievals is obtained, with a correlation coefficient of 0.96 and a normalized root mean squared error of 8 %. A slightly worse agreement is found for 27 July 2010, with a correlation coefficient of 0.64 and a normalized root mean squared error of 46 %, nonetheless the linear correlation is still significant for a 95 % confidence interval. In fact on 27 July 2010, a minor desert dust transport event was starting to affect the area, with aerosol optical depths (at 440 nm) that reached 0.26, whereas for clean background situations the aerosol optical depth at 440 nm is lower than 0.12 (Elias et al., 2006). In these cases the atmospheric conditions can hardly be considered spatially homogeneous,

HESSD
8, 11357–11385, 2011

therefore the situation between Évora (where the aerosol measurements are taken) and Alqueva may be somewhat different and the atmospheric correction results reflect this. On 24 February 2011, MERIS FR image data was not available due to issues connected with ESA acquisition strategy, therefore the satellite image used in this campaign is the MERIS reduced resolution (1200 m at nadir). The major problems arising in this case are mainly connected to pixel dimension and since Alqueva is not a very large lake, the difficulties associated with adjacency effects increase. Nevertheless, a correlation coefficient of 0.87 and a normalized root mean squared error of 16 % are found. To sum up, the overall results for the 89 data points available from the three field campaigns are quite promising with a rather low intercept of 0.005 and a slope of 0.86, a correlation coefficient of 0.84, a root mean squared error (RMSE) of 0.007 and a normalized root mean squared error (NRMSE) of 14 % (Table 2).

Figure 3b shows the campaign results as a whole (MERIS L1 + 6S), as well as the corresponding values obtained from MERIS Lake algorithm referred to as MERIS ATBD and with MERIS level 2 product. Table 2 summarizes the statistical parameters of the regressions obtained for each of the three atmospheric correction methods considered. It can be noted that the atmospheric correction applied according to the methodology proposed by Potes et al. (2011) (MERIS L1 + 6S) presents the best fit with FieldSpec measurements, with a correlation coefficient of 0.84, whereas both MERIS L2 and ATBD present pretty low correlation coefficients of 0.27 and −0.21, respectively. Also the NRMSE values for the latter two methods (33 and 27 %) are about twice the value obtained for MERIS L1 + 6S, which is of 14 %. These results hint to the need for a specific atmospheric correction in Alqueva area, allowing the use of water leaving spectral reflectances to accurately estimate water quality related parameters.

2.2 Empirical algorithm

The retrieved water leaving spectral reflectance is related with water turbidity in situ measurements, using the atmospherically corrected satellite data in combination with

HESSD
8, 11357–11385, 2011

the corresponding limnological data (Sathyendranath, 2000; Bukata et al., 1995). This kind of technique was proposed before by Koponen et al. (2002) to monitor water turbidity in Finnish Lakes and Chen et al. (2006) has applied a similar methodology in Tampa Bay (Florida, USA).

The data used for this purpose refers to the period 2007–2008. The best retrieval algorithm was found empirically by deriving a regression model for all possible channels and channel ratio combinations and selecting the one with the highest correlation coefficient. The algorithms proposed by Chen (2006), Koponen (2002) and Härmä (2001) found in the red and near infrared spectral bands the best fits and consequently the empirical algorithms to retrieve water turbidity. Yet, in this study, the best fit found uses a ratio between green and blue spectral regions. The sensitivity to different spectral regions may be explained by the characteristics of the turbidimeter employed to measure water turbidity in Alqueva, which uses a tungsten lamp operating between 400 and 600 nm, the same spectral range found to be the best combination for the empirical algorithm. The best fit between in situ water turbidity and atmospherically corrected satellite spectral reflectance combination revealed to be of linear type, using the ratio between the green (560 nm) and blue (412.5 nm) MERIS spectral bands, with a rather high correlation coefficient of 0.96 (Fig. 4). A total number of 17 data points is used, corresponding to the two locations considered (Fig. 1) and to the period of study, taking into account the conditions imposed for the MERIS image selection (cloud-free sky, lack of aerosol events and minimum time lag between MERIS and limnology dates).

To emphasize that the highest turbidity point of almost 60 NTU (Fig. 4) plays an important role in the linear correlation found (0.96), nevertheless if the referred point is removed from the dataset, the linear correlation is still significant for a 99 % confidence interval ($R = 0.82$). The empirical algorithm obtained is then used to estimate the water turbidity over the whole Alqueva reservoir surface area, as exemplified in Sect. 3.

Several authors propose different equations relating water turbidity and extinction coefficients (Giblin et al., 2010; Parkhill and Gulliver, 2002; Oliver et al., 1999; Roos and Pieterse, 1994; Grobler et al., 1983; Lloyd et al., 1987). Nine different relationships

Discussion Paper | Discussion Paper | Discussion Paper | Discussion Paper |

HESSD

8, 11357–11385, 2011

Satellite remote sensing of water turbidity in Alqueva reservoir

M. Potes et al.

were analyzed (eight linear and one of quadratic type) and applied to the turbidity measurements taken in Alqueva reservoir in order to estimate the extinction coefficients. The minimum and maximum mean values obtained were of 1.0 and 6.1 m^{-1}, respectively, with greater dispersion found for the upper limit of the water extinction coefficients estimated, hence, the sensitivity study was conducted using these two values as lower and upper limits. Although these values are obtained for different conditions than those of Alqueva reservoir, they represent typical values of extinction coefficients for clean and turbid waters, indicating possible minimum and maximum values expected for Alqueva, thus are deemed suitable to carry on a sensitivity analysis on the surface water temperature and water-atmosphere heat fluxes.

2.3 FLake model

The FLake model, fully documented in Mironov (2008), is intended for use as a lake parameterization scheme in numerical weather prediction, climate modelling, and other numerical prediction systems for environmental applications. It is based on a two-layer representation of the evolving temperature profile and on the integral energy budgets for the two layers. The structure of the stratified layer between the upper mixed layer and the basin bottom, the lake thermocline, is described using the concept of self-similarity of the temperature-depth curve. With this assumption, the water temperature profile is completely described by four variables: the mixed-layer surface temperature, T_S, the temperature at the lake bottom, T_{BOT}, the thickness of the mixed-layer, h, and the shape factor C_T; and one fixed parameter: the lake depth, D, $(D-h)$ is the thermocline depth.

In order to solve the energy balance equations for the two layers, the short-wave radiative flux is computed using the exponential approximation of the decay law (Eq. 1). The light extinction coefficient in water (k in Eq. 1), similarly to other optical characteristics of water, is lake-specific and time dependent and should hence be estimated with caution in every particular case. Up to 8 spectral bands characterized by different extinction coefficients may be considered in FLake.

HESSD
8, 11357–11385, 2011

The FLake model also includes optional schemes for the representation of upper layers of ice and snow and a bottom layer of sediments. The first ones were not activated in the present work as lake waters do not freeze in the region. The evolution of the vertical temperature structure of the thermally active layer of bottom sediments is computed using the same concept of self-similarity.

3 Case study results

A nearly continuous precipitation event that occurred during January and first week of February 2009 (Fig. 5) in the south of Portugal, with roughly 210 mm of accumulated precipitation in 41 days, was recorded in Évora – Verney Meteorological station (Évora Geophysics Centre). Strong and continuous precipitation in the area causes a run-off, mainly by the Guadiana River, which usually introduces organic and inorganic matter in Alqueva reservoir, leading to an increase of water turbidity.

This effect is explored in the maps of turbidity shown in Fig. 6a,b, obtained applying the developed algorithm (Fig. 4) to the whole Alqueva reservoir area. It can be clearly noticed that on 11 February 2009 (just after the precipitation event) the reservoir presents in general, high turbidity values (>30 NTU) in comparison with the results obtained for 15 March 2009 (1 month after the precipitation event), where the lake presents rather low turbidity values (<10 NTU).

These results constitute a strong indication that the empirical algorithm derived provides meaningful turbidity values. Further turbidity measurements, which are not available presently, will consent to extend the turbidity limits, to strengthen the correlation and to validate the empirical algorithm.

HESSD
8, 11357–11385, 2011

4 FLake sensitivity to the extinction coefficient of sunlight

In order to investigate is the importance of turbidity in the evolution of the lake surface water temperature, a sensitivity test of the FLake model to the water extinction coefficient was conducted.

The test consisted of FLake off-line simulations forced by atmospheric data collected at the Alqueva reservoir, using typical minimum and maximum expected extinction coefficients of 1.0 m^{-1} (clear water) and 6.1 m^{-1} (turbid water).

The model runs are carried out for May and June 2007 (61 days). In this period, the water thermal profile is stratified. The forcing consists of time series of the hourly averaged meteorological variables – pressure, air moisture and temperature, wind speed and solar global radiation – collected at the Mourão meteorological station. This station belongs to the Portuguese Water Institute (INAG) and is installed on a floating platform located near Mourão site (see Salgado and Le Moigne, 2010, for a description of this type of stations). The data are available at the site http://snirh.pt. Since the downward longwave radiation flux is not measured at the station, though it is also needed, it was obtained from linear interpolation of the 3-hourly output of the ECMWF IFS weather forecast model.

The initial conditions were constructed from hourly water temperature observations collected at the same point. Unfortunately, the water temperature measurements are only available at 3 levels (surface, middle and bottom), which are not sufficient to adjust a FLake initial profile, which is characterized by four variables. Thus, only the initial bottom temperature and the surface mixed layer temperature were tacked directly from the observations. The other initial values (C_T and h) were obtained by tuning the model to reproduce the measured water surface temperature dataset. Due to the complex topographical characteristics of the artificial reservoir, the lake depth, D, which is not a local but an effective or spatially-averaged parameter, was also estimated by the tuning workout. In the tuning simulations, the value of the extinction coefficient corresponding to turbid water ($k = 6.1\,m^{-1}$) was imposed. After this procedure, the following

Discussion Paper | Discussion Paper | Discussion Paper | Discussion Paper |

HESSD

8, 11357–11385, 2011

Satellite remote sensing of water turbidity in Alqueva reservoir

M. Potes et al.

Title Page
Abstract Introduction
Conclusions References
Tables Figures
◀◀ ▶▶
◀ ▶
Back Close
Full Screen / Esc
Printer-friendly Version
Interactive Discussion

parameters and initial conditions were used: $D = 23\,\text{m}$, $T_S = 290.6\,\text{K}$, $T_{BOT} = 287.5\,\text{K}$, $h = 4\,\text{m}$, $C_T = 0.79$.

Model runs for 61 days with a time step of 30 min. The initial conditions, the lake depth and the forcing were the same for all the simulations, which only differ on the extinction coefficient. Only the two extreme cases, corresponding to turbid and clear water values, of $k = 6.1\,\text{m}^{-1}$ (simulation Mo61) and $k = 1.0\,\text{m}^{-1}$(simulation Mo10), will be analyzed and discussed. In the following, the simulations will be identified, respectively by Mo61 and Mo10.

As expected and shown in Fig. 7a,b, the simulation Mo61 reproduces better the water surface diurnal cycle on June 6 (the day when it was recorded the highest turbidity value), In particular the modeled daily amplitude (around 2 °C) is closed to the observed one and higher than that obtained in the Mo10 (around 1 °C). In the late afternoon and evening, the observed water surface temperature dropped sharply due to the occurrence of strong wind, a feature not fully represented by the model, even in Mo61 simulation.

The lower the coefficient of the extinction, the lower the daily temperature range is. This is visible on this particular day, but also during the entire period, as shown in Fig. 7c,d. The respective Figures shows that surface temperature variations are more sudden in the Mo61 simulation. This is not an unexpected result, since when the water is more turbid, solar radiation will penetrate less deeply and therefore will be more absorbed in the surface layer, heating it.

The results show that there are periods when the observed evolution is better reproduced by the simulation Mo61 (the first 10 days, for example), while by contrast, others are better represented in the Mo10, corresponding to days with less thermal amplitude (days 45 to 55, for example). It is possible that the periods best represented by the Mo61 experience correspond to days of higher water turbidity and vice versa. Unfortunately we lack a turbidity time series in order to confirm this assumption.

In any case, it can be concluded that the model is very sensitive to the extinction coefficient and that variations in turbidity (within the range of observed values) can lead

HESSD
8, 11357–11385, 2011

to important differences in the lake surface temperature, which is a relevant parameter for heat and moisture transfers between water bodies and the atmosphere. Under the conditions assumed in the present sensitivity test, the daily mean surface temperature range jumps from of about 1.2 °C in the Mo10 (with a maximum of about 2.8 °C) to 2.4 °C in the Mo61 (with a maximum of about 5.3 °C).

These differences in surface temperature have effects in the patterns of surface sensible heat flux, H and evaporation, E. For the whole simulation period, the increase in simulated sensible heat flux between Mo10 and Mo61 is of about 7 %. The simulated difference in total evaporation is relatively smaller, with the evaporation being about 3 % higher for the simulation with higher turbidity (Mo61). The results thus indicate that more turbid lake waters tend, during the heating season, to prevent heating of the whole water column (leading to less heat storage) and transfer the energy faster to the atmosphere, resulting in a colder lake. In the end of the simulation period, the column mean water temperature is 0.3 °C higher in Mo10 than in Mo61.

5 Conclusions

A satellite based methodology was developed and applied to retrieve the surface water turbidity of Alqueva reservoir, in the south of Portugal. An important aspect of the satellite data use for surface applications is the atmospheric correction process. A validation of the atmospheric correction is presented, based on the comparison between ground based and atmospherically corrected spectral reflectance measurements, obtained during three field campaigns carried out in Alqueva throughout 2010 and early 2011. A correlation coefficient of 0.84 and a NRMSE of 14 % are obtained for the comparison, which are deemed adequate, especially when compared to different atmospheric correction algorithms that are probably not suited for Alqueva lake area.

The empirical algorithm proposed to estimate surface water turbidity from atmospherically corrected satellite spectral reflectance is of linear type and combines green (560 nm) and blue (412.5 nm) spectral regions, presenting a high correlation coefficient

HESSD
8, 11357–11385, 2011

of 0.96. Since only 17 data point were available for the study, new field campaigns are planned for Alqueva reservoir, including turbidity as well as spectral reflectance and light extinction measurements. This is aimed at strengthening the confidence on the turbidity algorithm proposed, extend the turbidity limits and derive a proper relation for the Alqueva lake extinction coefficient. Nevertheless, the turbidity spatial distribution obtained for the whole lake, for a case study, provided meaningful results.

A sensitivity study of the FLake model to the water extinction coefficient was also conducted in order to investigate the importance of turbidity in the evolution of the lake surface water temperature. Results show that the model is very sensitive to different extinction coefficient values and that variations in turbidity can lead to significant changes in the lake surface temperature, which is a parameter that plays a central role in heat and moisture transfers between the lake and the atmosphere. The results also indicate that the turbidity of water should be taken into account in lake schemes inside high-resolution weather forecast models. While it is not possible to include this parameter in the assimilation systems, we suggest the setup of time-dependent global climatological maps of the light extinction coefficient of lake waters to be used by the forecast models. Those maps may be built following the satellite based methodology described in this work.

Acknowledgements. This work is financed through FEDER (Programa Operacional Factores de Competitividade – COMPETE) and National funding through FCT – Fundação para a Ciência e a Tecnologia in the framework of projects FCOMP-01-0124-FEDER-007122 (PTDC/CTE-ATM/65307/2006) and FCOMP-01-0124-FEDER-009303 (PTDC/CTE-ATM/102142/2008) and through FCT grant SFRH/BD/45577/2008. Image data has been provided by ESA in the frame of ENVISAT projects AOPT-2423 and AOPT-2357. We thank AERONET investigators for their effort in establishing and maintaining Évora AERONET site. We also thank the Water Laboratory of the University of Évora for support in the field campaigns and EDIA for providing the water quality data used in this work. We are grateful to the Portuguese Institute of Meteorology and ECMWF for MARS database account.

References

Alikas, K. and Reinart, A.: Validation of the MERIS products on large European lakes: Peipsi, Vänern and Vättern, Hydrobiologia, 599, 161–168, 2008.

Bukata, R. P., Jerome, J. H., Kondratyev, K. Y., and Pozdnyakov, D. V.: Optical Properties and Remote Sensing of Inland and Coastal Waters, CRS Press, 135–250, 1995.

Chapman, D.: Water Quality Assessments: a Guide to the Use of Biota, Sediments and Water in Environmental Monitoring, 2nd Edn., Chapman & Hall, London, 626 pp., 1996.

Chen, Z., Hu, C., and Muller-Karger, F.: Monitoring turbidity in Tampa Bay using MODIS/Aqua 250-m imagery, Remote Sens. Environ., 109, 207–220, 2006.

Dickey, T., Lewis, M., and Chang, G.: Optical oceanography: recent advances and future directions using global remote sensing and in situ observations, Rev. Geophys., 44, RG1001/2006, doi:10.1029/2003RG000148, 2006.

Doerffer, R. and Schiller, H.: MERIS Regional Coastal and Lake Case 2 Water Project – Atmospheric Correction ATBD, GKSS Research Center 21502 Geesthacht Version 1.0, 2008.

Duan, H., Zhang, Y., Zhang, B., Song, K., Wang, Z., Liu, D., and Li, F.: Estimation of chlorophyll-a concentration and trophic states for inland lakes in Northeast China from Landsat TM data and field spectral measurements, Int. J. Remote Sens., 29, 767–786, 2008.

Dutra, E., Stepanenko, V. M., Balsamo, G., Viterbo, P., Miranda, P. M. A., Mironov, D., and Schär, C.: An offline study of the impact of lakes on the performance of the ECMWF surface scheme, Boreal Environ. Res., 15, 100–112, 2008.

Elias, T., Silva, A. M., Belo, N., Pereira, S., Formenti, P., Helas, G., and Wagner, F.: Aerosol extinction in a remote continental region of the Iberian Peninsula during summer, J. Geophys. Res., 111, D14204, doi:10.1029/2005JD006610, 2008.

ESA: MERIS Product Handbook, Issue 2.0, available online at: http://envisat.esa.int/handbooks/meris/, last access: March 2008.

Friedl, G. and Wüest, A.: Disrupting biogeochemical cycles, Consequences of damming, Aquat. Sci., 64, 55–65, 2002.

Giblin, S., Hoff, K., Fischer, J., and Dukerschein, T.: Evaluation of light penetration on Navigation Pools 8 and 13 of the Upper Mississippi River, US Geological Survey Long Term Resource Monitoring Program Technical Report 2010–T001, 26 pp., 2010.

Gitelson, A. A., Dall'Olmo, G., Moses, W., Rundquist, D. C., Barrow, T., Fisher, T. R., Gurlin, D., and Holz, J.: A simple semi-analytical model for remote estimation of chlorophyll-*a* in turbid waters: validation, Remote Sens. Environ., 112, 3582–3593, 2008.
Gons, H. J., Auer, M. T., and Effler, S. W.: MERIS satellite chlorophyll mapping of oligotrophic and eutrophic waters in the Laurentian Great Lakes, Remote Sens. Environ., 112, 4098–4106, 2008.
Gordon, H. R. and Wang, M.: Retrieval of water-leaving radiance and aerosol optical thickness over the oceans with SeaWiFS: a preliminary algorithm, Appl. Optics, 33, 443–452, 1994.
Grobler, D. C., Toerien, D. F., and De Wet, J. S.: Changes in turbidity as a result of mineralization in the lower Vall River, Water SA, 9, 263–266, 1983.
Härmä, P., Vepsäläinen, J., Hannonen, T. P., Kämäri, J., Kallio, K., Eloheimo, K., and Koponen, S.: Detection of water quality using simulated satellite data and semi-empirical algorithms in Finland, Sci. Total Environ., 268, 107–121, 2001.
Holben, B. N., Tanre, D., Smirnov, A., Eck, T. F., Slutsker, I., Abuhassan, N., Newcomb, W. W., Schafer, J., Chatenet, B., Lavenue, F., Kaufman, Y. J., Vande Castle, J., Setzer, A., Markham, B., Clark, D., Frouin, R., Halthore, R., Karnieli, A., O'Neill, N. T., Pietras, C., Pinker, R. T., Voss, K., and Zibordi, G.: An emerging ground-based aerosol climatology: aerosol optical depth from AERONET, J. Geophys. Res., 106, 12067–12097, 2001.
Koponen, S., Pulliainen, J., Kallio, K., and Hallikainen, M.: Lake water quality classification with airborne hyperspectral spectrometer and simulated MERIS data, Remote Sens. Environ., 79, 51–59, 2002.
Lee, R. W. and Walter, R.: Light attenuation in a shalloe, turbid reservoir, lake Houston, Texas, US Geological Survey, Water-Resources Investigations Report 97-4064, 1997.
Lloyd, D. S., Koenings, J. P., and Laperriere, J. D.: Effects of turbidity in fresh waters of Alaska, N. Am. J. Fish. Manage., 7, 18–33, 1987.
Michaud, J. P.: A citizen's guide to understanding and monitoring lakes and streams, Publ. #94–149, Washington State Dept. of Ecology, Publications Office, Olympia, WA, USA, 360, 407–7472, 1991.
Mironov, D., Rontu, L., Kourzeneva, E., and Terzhevik, A.: Towards improved representation of lakes in numerical weather prediction and climate models: Introduction to the special issue of Boreal Environment Research, Boreal Environ. Res., 15, 97–99, 2010.

HESSD
8, 11357–11385, 2011

Mironov, D. V.: Parameterization of lakes in numerical weather prediction. Description of a lake model, COSMO Technical Report 11, Deutscher Wetterdienst, Offenbach am Main, Germany, 41 pp., 2008.
Moore, G. K.: Satellite remote sensing of water turbidity, Hydrolog. Sci. J., 25, 407–421, 1980.
Morais, M., Serafim, A., Pinto, P., Ilhéu, A., and Ruivo, M.: Monitoring the water quality in Alqueva reservoir, Guadiana River, Southern Portugal, Reservoir and River Basin Management, Exchange of Experiences from Brazil, Portugal and Germany, edited by: Gunkel, G. and Sobral, M., Technical University of Berlin, Berlin, 96–112, 2007.
Oliver, R. L., Hart, B. T., Olley, J., Grace, M., Rees, C., and Caitcheon, G.: The Darling River: Algal Growth and the Cycling and Sources of Nutrients, Final report to the Murray-Darling Basin Commission, 1999.
Parkhill, K. L. and Gulliver, J. S.: Effect of inorganic sediment on whole stream productivity, Hydrobiologia, 472, 5–17, 2002.
Potes, M., Costa, M. J., Silva, J. C. B., Silva, A. M., and Morais, M.: Remote sensing of water quality parameters over Alqueva reservoir in the south of Portugal, Int. J. Remote Sens., 32, 3373–3388, 2011.
Roos, J. C. and Pieterse, J. H.: Light, temperature and flow regimes of the Vaal River at Balkfontein, South Africa, Hydrobiologia, 277, 1–15, 1994.
Salgado, R. and Le Moigne, P.: Coupling of the FLake model to the Surfex externalized surface model, Boreal Environ. Res., 15, 231–244, 2010.
Sathyendranath, S.: Remote sensing of ocean colour in coastal, and other optically-complex, waters, in: Reports of the International Ocean-Colour Coordinating Group, No. 3, IOCCG, Dartmouth, Canada, 2000.
Simis, S., Ruiz-Verdú, A., Domínguez-Gómez, J. A., Peña-Martinez, R., Peters, S., and Gons, H. J.: Influence of phytoplankton pigment composition on remote sensing of cyanobacterial biomass, Remote Sens. Environ., 106, 414–427, 2007.
Tyler, A. N., Svab, E., Preston, T., Preacutesing, M., and Kovaacutecs, W. A.: Remote sensing of the water quality of shallow lakes: A mixture modelling approach to quantifying phytoplankton in water characterized by high-suspended sediment, Int. J. Remote Sens., 27, 1521–1537, 2007.
Vermote, E. F., Tanré, D., Deuzé, J.-L., Herman, M., and Morcrette, J.-J.: Second simulation of the satellite signal in the solar spectrum: An overview, IEEE T. Geosci. Remote, 35, 675–686, 1997.

HESSD
8, 11357–11385, 2011

Title Page
Abstract | Introduction
Conclusions | References
Tables | Figures
◂◂ | ▸▸
◂ | ▸
Back | Close
Full Screen / Esc
Printer-friendly Version
Interactive Discussion

Table 1. Parameters obtained in the correlation between the measured and satellite-derived water leaving spectral reflectance (MERIS L1 + 6S) for the three field campaigns carried out. The parameters are the following: number of data (N), equation of the regression, correlation coefficients (R), root mean squared errors (RMSE) and normalized root mean squared errors (NRMSE).

Campaign date	N	Regression equation	R	RMSE	NRMSE (%)
27 Jul 2010	14	$0.73x + 0.012$	0.64	0.01	46
25 Aug 2010	30	$1.04x - 0.0007$	0.96	0.002	8
24 Feb 2011	45	$0.77x + 0.008$	0.87	0.007	16

HESSD
8, 11357–11385, 2011

Table 2. Parameters obtained in the correlation between the measured and satellite-derived water leaving spectral reflectance for the three methods that are compared. The parameters are the same as in Table 1.

Method	N	Regression equation	R	RMSE	NRMSE (%)
MERIS L1 + 6S	89	$0.86x+0.005$	0.84	0.007	14
MERIS L2	78	$0.28x-0.0003$	0.27	0.02	33
MERIS ATBD	72	$-0.08x+0.006$	−0.21	0.012	27

Discussion Paper | Discussion Paper | Discussion Paper | Discussion Paper |

HESSD
8, 11357–11385, 2011

Satellite remote sensing of water turbidity in Alqueva reservoir

M. Potes et al.

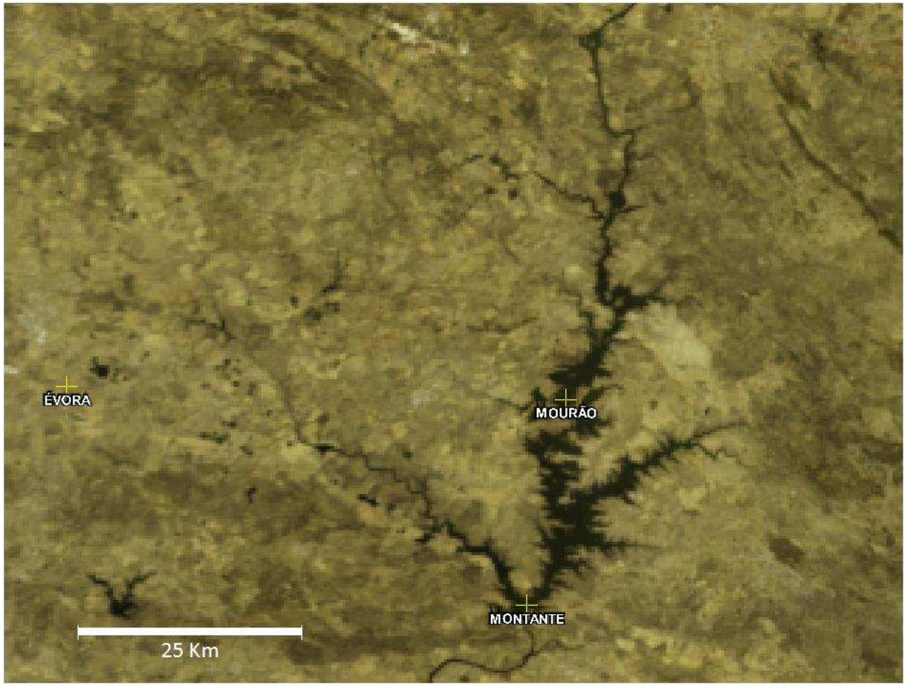

Fig. 1. MERIS image showing Alqueva reservoir location and position of the sites used in the study. The city of Évora is also indicated as a point of reference.

HESSD
8, 11357–11385, 2011

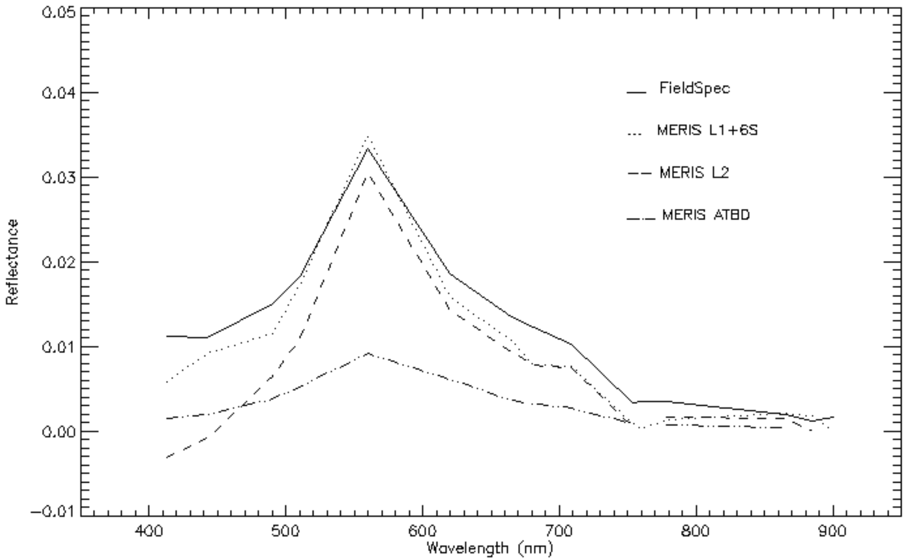

Fig. 2. Comparison between the measured and satellite-derived water leaving reflectance spectra on 25 August 2010 in Montante site. The measured spectra are identified as FieldSpec (solid line) and the satellite-derived are MERIS L1 + 6S (dotted), MERIS L2 (dashed) and MERIS ATBD (dash dot dot).

HESSD
8, 11357–11385, 2011

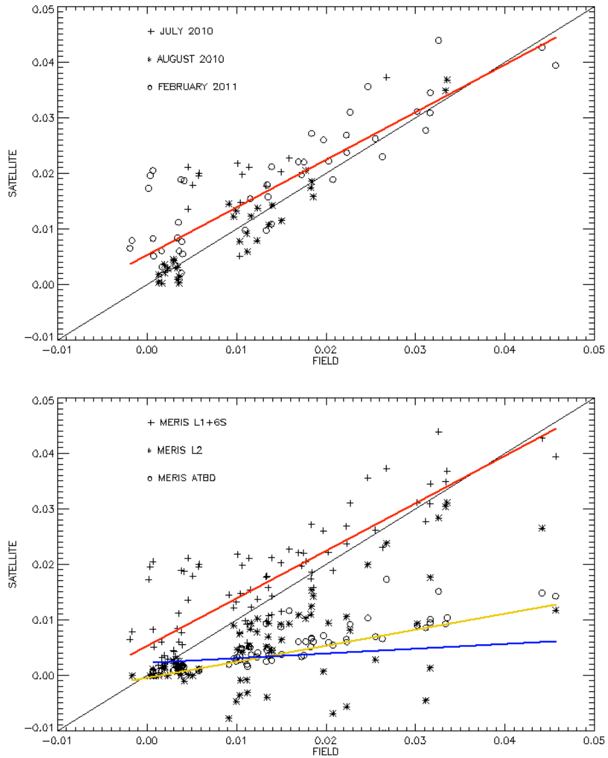

Fig. 3. Scatter plot of the measured versus satellite-derived water leaving spectral reflectance: **(a)** obtained for the three field campaigns carried out, distinguished by the different symbols, considering only the MERIS L1 + 6S retrieval versus the field measurements and **(b)** obtained from the three methods that are compared.

HESSD
8, 11357–11385, 2011

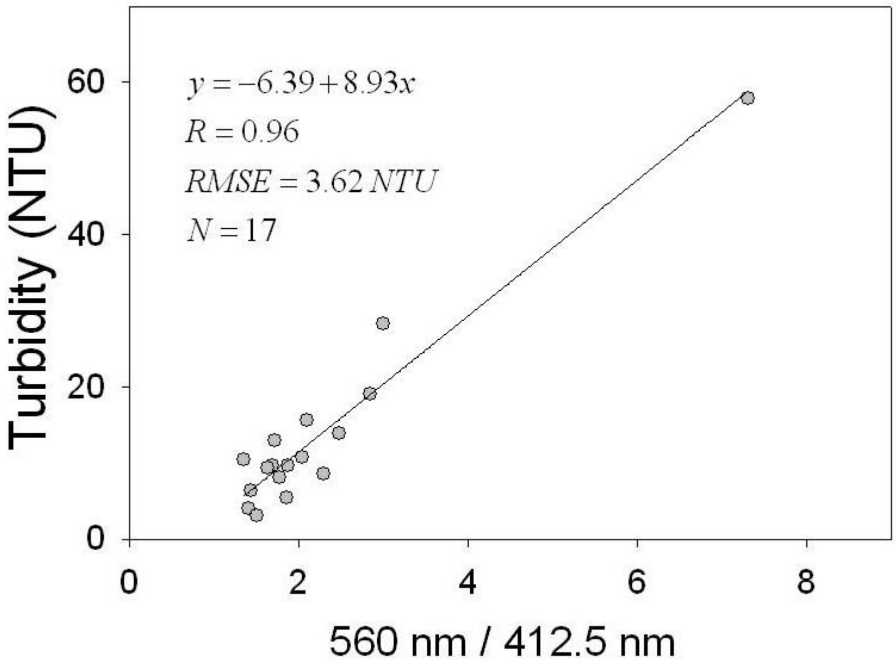

Fig. 4. Scatter plot between water turbidity (NTU) and the ratio between MERIS band 5 (560 nm) and band 1 (412.5 nm). Also shown the linear regression obtained.

HESSD
8, 11357–11385, 2011

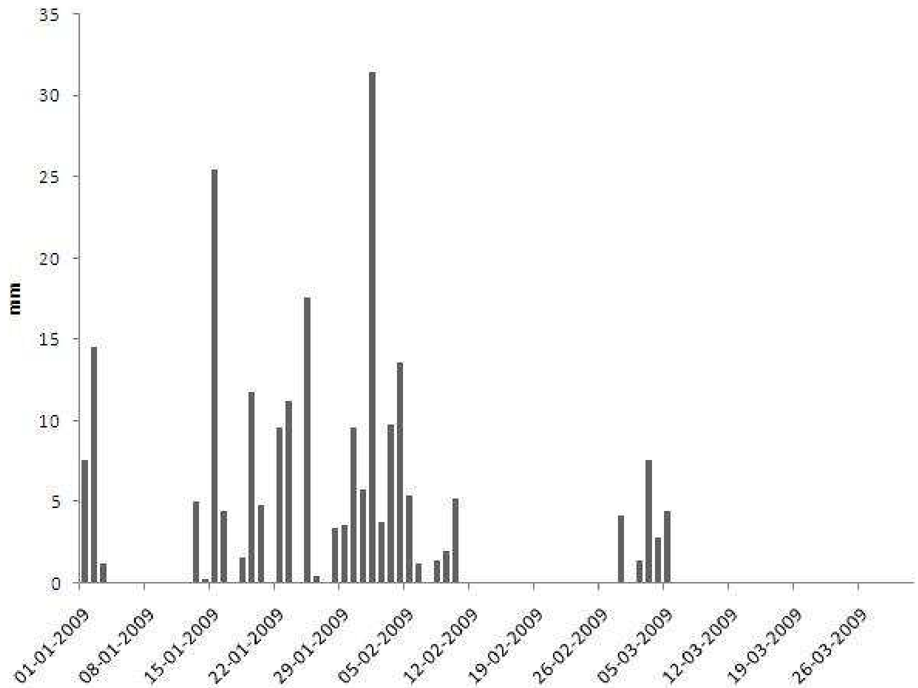

Fig. 5. Daily precipitation recorded in Évora Geophysics Centre, from January to March 2009.

HESSD
8, 11357–11385, 2011

Title Page
Abstract Introduction
Conclusions References
Tables Figures
◀I ▶I
◀ ▶
Back Close
Full Screen / Esc
Printer-friendly Version
Interactive Discussion

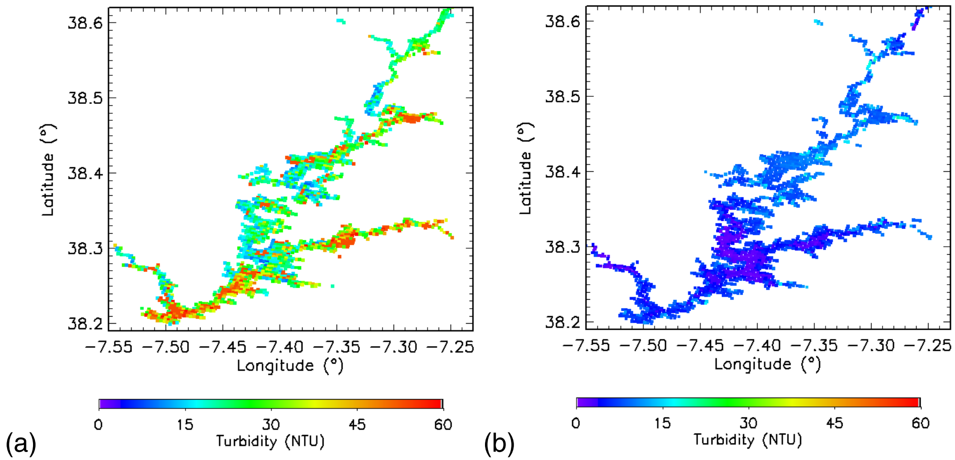

Fig. 6. Turbidity maps for Alqueva reservoir on **(a)** 11 February 2009 and **(b)** 15 March 2009.

HESSD
8, 11357–11385, 2011

Satellite remote sensing of water turbidity in Alqueva reservoir

M. Potes et al.

Title Page
Abstract Introduction
Conclusions References
Tables Figures
◀| |▶
◀ ▶
Back Close
Full Screen / Esc
Printer-friendly Version
Interactive Discussion

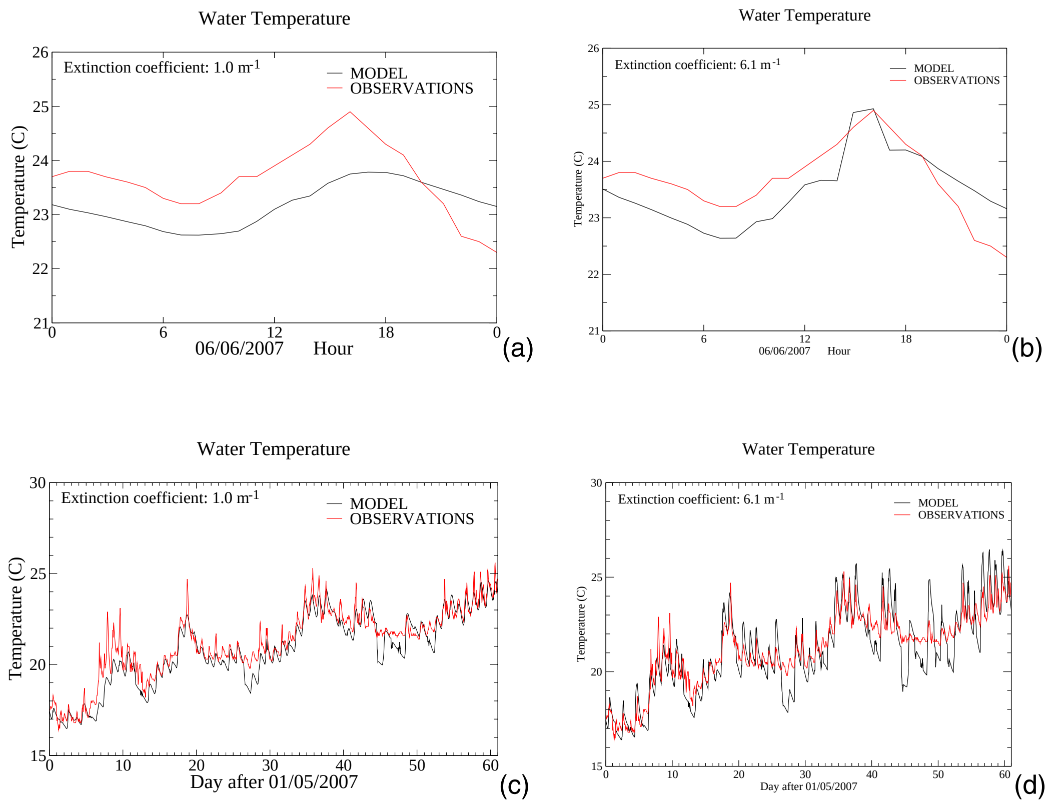

Fig. 7. Comparison between the lake water surface temperature observed and modeled with FLake for: **(a)** 6 June 2007 with an extinction coefficient of 1.0 m^{-1} (simulation Mo10); **(b)** 6 June 2007 with an extinction coefficient of 6.1 m^{-1} (simulation Mo61); **(c)** May and June 2007 with an extinction coefficient of 1.0 m^{-1} (simulation Mo10); **(d)** May and June 2007 with an extinction coefficient of 6.1 m^{-1} (simulation Mo61).

HESSD
8, 11357–11385, 2011